

VERIFICATION OF THE MATERIALS' PURITY WITH EDAX SPECTRUM AND ELEMENTAL ANALYSIS

¹DR Anuradha Gupta, ²Dr Arunbalaji, ³Sandhya Boosani

¹Professor, ^{2,3}Assistant Professor, ^{1,2,3}Department of Physics, Rishi MS Institute of Engineering and Technology for Women, Kukatpally, Hyderabad.

Abstract

Co-precipitated pure SnO₂ and Sn_{0.94}Cu_{0.02}Zn_{0.04}O₂ nanoparticles were created. PXRD investigation of the structural characteristics revealed that the produced samples are in the nanoscale range. The structure of all synthesized samples is tetragonal. All of the samples' aggregated nanoparticles may be seen by SEM morphology. The EDAX spectrum verified the elemental analyses and attested to the materials' cleanliness. By using FTIR measurement, Sn-Cu-Zn-chemical O's bonding was confirmed. By using photoluminescence spectroscopy, oxygen vacancies and surface flaws created during the synthesis process are identified.

Keywords: pure snO₂, sn_{0.9}cu_{0.02}zn_{0.04}o₂, nanoparticles, PXRD investigation, EDAX spectrum, FTIR measurement

1. Introduction

A variety of fundamental categories of useful materials, including polymers, magnetic, dielectric, and semiconductors, are available. Due to their exceptional characteristics, semiconductors are among the most fascinating materials. Numerous semiconductor oxides were available, including FeO [1], TiO₂ [2], CuO [3], NiO [4], SnO₂ [5], and PbO [6]. Their extensive and intriguing features have sparked interest in these materials for study. SnO₂, an n-type semiconductor oxide (E_g=3.6 eV) in the midst of these, is projected to have a variety of uses in photodetectors [7], catalysis [8], gas sensors [9], transparent conducting electrodes [10], solar cells [11], rechargeable Li-batteries [12], and optoelectronic instruments. [13].

There are a few systems for the synthesis of SnO₂ nanoparticles, for example, spray pyrolysis [14], laser removal procedure [15], sol-gel [16], wet chemical method [17], co-precipitation [18], hydrothermal [19], strong state calcination [20]. Most importantly, co-precipitation has, for the most part, utilized as a strategy to combine SnO₂ nanoparticles due to its simplicity, high capability, and minimal effort.

Doping is a procedure that assists in enhancing the benefits of semiconductors. It guaranteed that the immediate exchange between the semiconductor oxides with doping particles make changes from their characteristic property. SnO₂ nanoparticles have viably doped with a few TM (Transition Metal) particles, for example, Cu [21], Ni [22], Mn [23], Fe [24], Co [25], Cd [26] and Mg [27] that acquires a surprising change the SnO₂ nanoparticles.

Among these transition metal ions, Cu and Zn are concentrating on this work due to its fascinating property. Also, the Cu doped SnO₂ nanoparticles and the stunning expressions were discussed elaborately [28, 29]. From these results, it proved that Cu and Zn transition metal ions would be perfectly suitable for the SnO₂ doping process.

To make this article very captivating, we have arranged pure SnO₂ and (Cu and Zn) co-doped SnO₂ nanoparticles using the co-precipitation technique. The structural, morphological, elemental and optical qualities examined. The outcomes show that the (Cu and Zn)- co-doped particles bring a significant impact on the SnO₂, which drives the material to reasonable for optoelectronic devices.

2. Experimental Details

Chemicals

Tin chloride pentahydrate ($\text{SnCl}_2 \cdot 5\text{H}_2\text{O}$), Copper chloride dihydrate ($\text{CuCl}_2 \cdot 2\text{H}_2\text{O}$), Zinc chloride pentahydrate ($\text{ZnCl}_2 \cdot 5\text{H}_2\text{O}$) and Sodium hydroxide (NaOH) were used for the entire synthesis procedure. All the chemicals were obtained from sigma-aldrich (with 99% purity).

Preparation Method

Pure SnO_2 and $\text{Sn}_{0.94}\text{Cu}_{0.02}\text{Zn}_{0.04}\text{O}_2$ nanoparticles have incorporated by co-precipitation strategy. The appropriate measure of tin chloride pentahydrate ($\text{SnCl}_2 \cdot 5\text{H}_2\text{O}$), copper chloride dihydrate ($\text{CuCl}_2 \cdot 2\text{H}_2\text{O}$), and Zinc chloride pentahydrate ($\text{ZnCl}_2 \cdot 5\text{H}_2\text{O}$) dissolved into 50 ml D.D. water. This arrangement mixed for five hours, and then 2.16 g of NaOH included until it arrives at a specific PH level. Dark precipitated were collected and washed with ethanol. This washed precipitated was dried in an incubator for 12 hours and afterwards kept into the heater for 1 hr at 500°C .

Characterization Techniques

Crystalline nature and its structure confirmed by using Powder X-ray diffraction (PXRD) method. They instrumented by PAN analytical X'Pert, PRO diffractometer with $\text{Cu K}\alpha$ radiation ($\lambda = 1.5418 \text{ \AA}$). Shapes and ions presence of the nanoparticles confirmed through SEM (Carl Zeiss Model EVO18) and EADX (Amepek EDAX PV6500) analysis. Sn-Cu-Zn-O chemical bonds make assured from FTIR (Thermo Nicolet 380) spectroscopic analytical instrument. Structural defects and oxygen vacancies were affirm using Varian Cary Eclipse Photo Luminescence.

3. Results and Discussion

Powder X-Ray Diffraction Analysis

The pureness and crystalline structure of the synthesized samples assessed through the powder X-ray diffraction procedure. Figure 1 shows the diffraction peaks of (a) pure SnO_2 and (b) $\text{Sn}_{0.94}\text{Cu}_{0.02}\text{Zn}_{0.04}\text{O}_2$ nanoparticles. The diffraction patterns exposed that all the samples exhibit a tetragonal structure and match with JCPDS card No (41-1445). No individual peaks of different impurities influences were perceived, this means the prepared samples have high crystallinity and virtue. The crystallite size of the samples assessed utilizing the Debye-Scherrer recipe [30].

$$\text{The average crystallite size (D)} = \frac{0.9\lambda}{\beta \cos\theta} \quad (1)$$

Where λ , θ and β are the X-ray wavelength, Bragg diffraction point and full-width at half maximum, correspondingly.

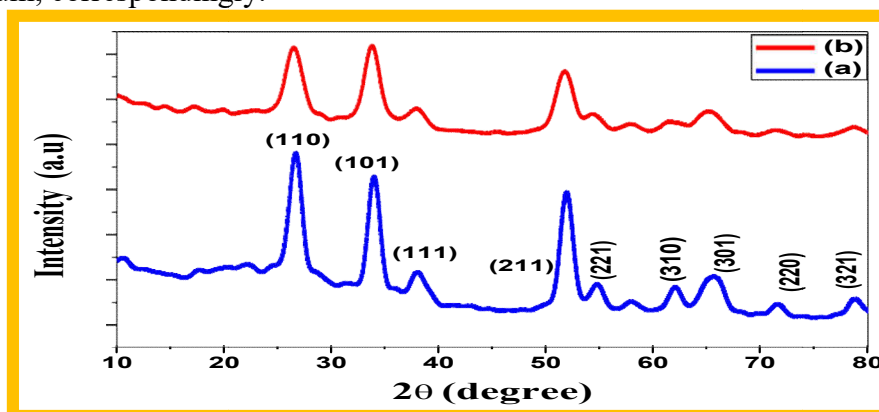


Figure 1: Powder X-ray diffraction patterns of (a) pure SnO_2 , (b) $\text{Sn}_{0.94}\text{Cu}_{0.02}\text{Zn}_{0.04}\text{O}_2$ nanoparticles.

The crystallite size decreases somewhat with expanding (Cu-2%, Zn-4%) concentration. The crystallite size for pure SnO₂ and Sn_{0.94}Cu_{0.02}Zn_{0.04}O₂ nanoparticles is 13 to 12 nm, respectively. Additionally PXRD pattern shows that 2θ of diffraction peak changes marginally to the lower angle, which recommends that Cu and Zn consolidation into the SnO₂ lattice. Micro-strain of the prepared nanoparticles determined by the following expression [31]. Table 1 gives the peak position, crystallite size, d-value, micro-strain, lattice parameter and unit Cell volume of (a) pure SnO₂ and (b) Sn_{0.94}Cu_{0.02}Zn_{0.04}O₂ nanoparticles.

$$\text{Micro-strain } (\epsilon) = \frac{\beta \cos \theta}{4} \quad (2)$$

Table 1. Peak Position, Average crystallite size (D), d-value, Micro-Strain (ε), Lattice parameter and Unit cell of (a) Pure SnO₂, (b) Sn_{0.94}Cu_{0.02}Zn_{0.04}O₂ nanoparticles.

| Samples | Peak Position, 2θ (deg) | Crystallite Size D (nm) | d- Values (Å) | Micro-Strain, ε (10 ⁻³) | Lattice parameters (Å) | | Unit Cell Volume (V) |
|---------|-------------------------|-------------------------|---------------|-------------------------------------|------------------------|--------|----------------------|
| | | | | | a=b | c | |
| A | 26.78 | 13 | 3.328 | 3.121 | 4.7071 | 3.1971 | 62.345 |
| B | 26.66 | 12 | 3.342 | 3.926 | 4.7263 | 3.2123 | 62.140 |

Surface Morphology Analysis

The morphology changes of the prepared nanoparticles analyzed by SEM examination. Figure 2 shows the exact morphological shapes of the prepared samples (a) pure SnO₂ and (b) Sn_{0.94}Cu_{0.02}Zn_{0.04}O₂ nanoparticles. Morphological pictures of both the samples show that readied nanoparticles are in the agglomerate state of the group.

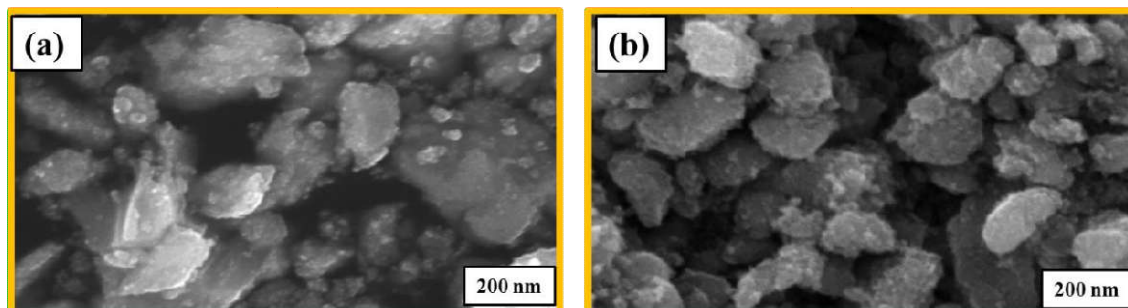


Figure 2: SEM image of (a) pure SnO₂, (b) Sn_{0.94}Cu_{0.02}Zn_{0.04}O₂ nanoparticles.

Figure 2 (a) shows the SEM pictures of pure SnO₂ nanoparticles that contain enormous and huge aggregate states of nanoparticles. For Sn_{0.94}Cu_{0.02}Zn_{0.04}O₂ nanoparticles the agglomerate shape increments and structure change into grain boundaries. These results affirmed that the readied samples are in the nanometer range and well crystalline nature. Furthermore, it means that (Cu-2%, Zn-4%) Co-doped ions have effectively modified the state of the SnO₂ nanoparticles.

Composition Analysis

A compositional investigation is important to screen the concentration of components existing of the prepared sample. Figure 3 (a and b) shows the EDAX spectra of pure SnO₂ and Sn_{0.92}Cu_{0.02}Zn_{0.04}O₂ nanoparticles. This EDAX examination existed that tin, oxygen, copper, and zinc components just with no different debasements. From figure 3 (a) we confirmed that only the pure SnO₂ nanoparticles was observed no impurities identified.

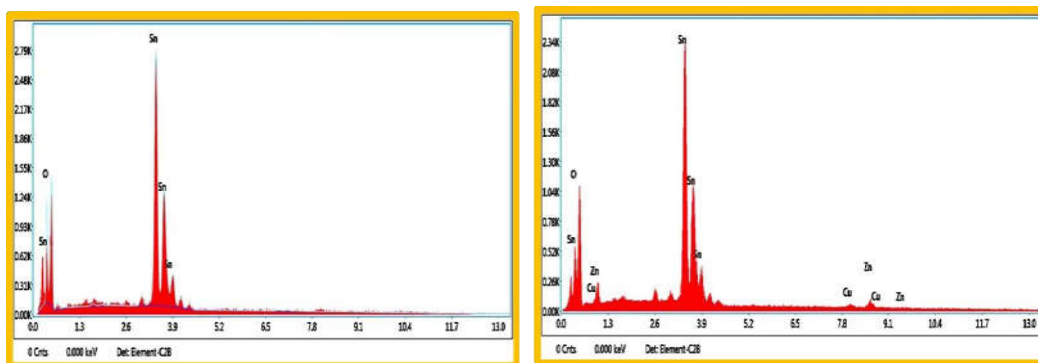


Figure 3: EDAX analysis of (a) pure SnO₂, (b) Sn_{0.94}Cu_{0.02}Zn_{0.04}O₂ nanoparticles.

For Sn_{0.94}Cu_{0.02}Zn_{0.04}O₂ nanoparticles, the atomic rates of Sn, O, Cu, and Zn components present in the as-synthesized powder are 38.60, 54.60, 2.50, and 4.30. The essential investigation of the pictures additionally demonstrated that prepared nanoparticles are marginally rich in Sn and O contrasted with Cu and Zn. The atomic weight percentage of each synthesis sample were given in Table 2.

Table 2. Weight percentage of (a) Pure SnO₂ and (b) Sn_{0.92}Cu_{0.02}Zn_{0.04}O₂ nanoparticles using EDAX analysis.

| Samples | Weight Percentage of the prepared Nanoparticles (%) | | | |
|---------|---|-------|------|------|
| | Sn | O | Cu | Zn |
| A | 41.81 | 58.19 | - | - |
| B | 38.60 | 54.60 | 2.50 | 4.30 |

Fourier Transform Infrared (FT-IR) Spectroscopy

Figure 4 shows the room temperature FT-IR transmission spectra of (a) pure SnO₂ and (b) Sn_{0.94}Cu_{0.02}Zn_{0.04}O₂ nanoparticles. Functional groups less than 1000 cm⁻¹ licensed to the vibrations of Sn-O and Zn-O obligation of the readied nanoparticles [32]. The peak begin at 647 cm⁻¹ identifies with the O-Sn-O connect a functional group of SnO₂, which affirms the presence of SnO₂ as a crystalline peak. This adjusts with the consequences of the PXRD investigation. From range, the peak focused at 1640-1650 cm⁻¹ found on the material assigned to O-H bending vibrations of a weakly-bounded water atom [33].

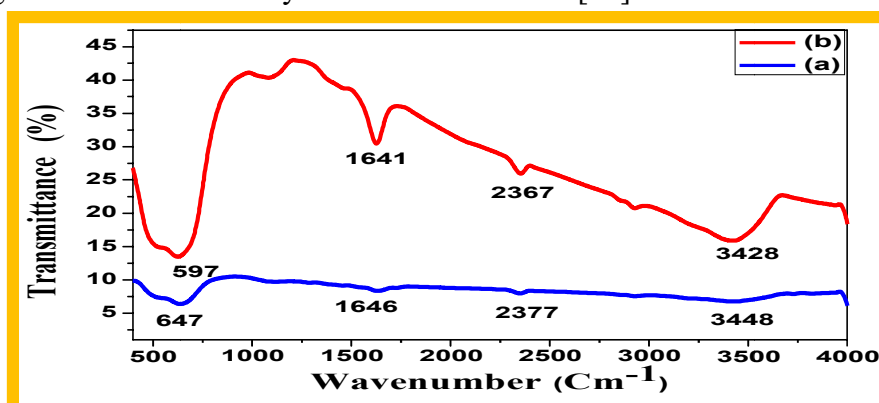


Figure 4: FT-IR spectrum of (a) pure SnO₂, (b) Sn_{0.94}Cu_{0.02}Zn_{0.04}O₂ nanoparticles.

The band at 2365-2380 cm⁻¹ determines the sign of environmental CO₂ from the environment [34]. The expansive consumed scale at 3448 and 3428 cm⁻¹, which is ascribed to

the vibration of a retained water particle and is consonant with the previous report [35, 36]. From this, we confirmed that the synthesized chemicals were successfully present.

photoluminescences spectroscopy

The PL outflow spectra give basic data about the surface imperfections, impurity influences, and exaction structure [37, 38]. Figure 5 shows the PL spectra of a) pure SnO_2 and b) $\text{Sn}_{0.94}\text{Cu}_{0.02}\text{Zn}_{0.04}\text{O}_2$ nanoparticles. Cause for the emanation properties is dependent on the combination strategy. The pure SnO_2 and $\text{Sn}_{0.94}\text{Cu}_{0.02}\text{Zn}_{0.04}\text{O}_2$ nanoparticles have comparative peak emissions. However, the peak intensity decreased for $\text{Sn}_{0.94}\text{Cu}_{0.02}\text{Zn}_{0.04}\text{O}_2$ nanoparticles. Quenching effect will be the purpose behind the decrease in peak intensity [39].

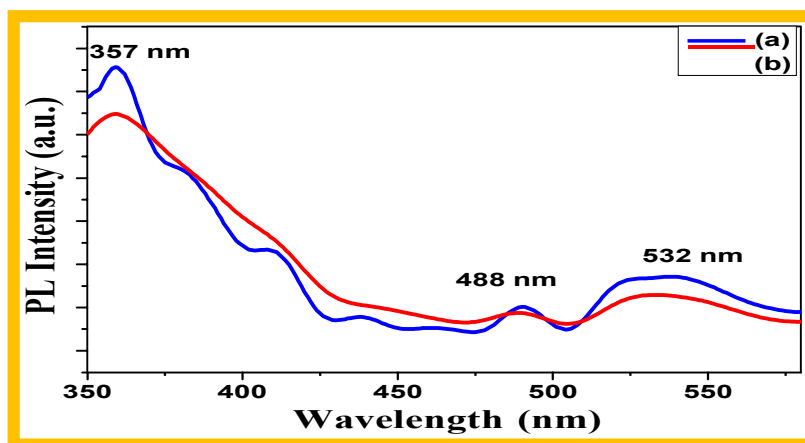


Figure 5: PL spectrum of (a) pure SnO_2 , (b) $\text{Sn}_{0.94}\text{Cu}_{0.02}\text{Zn}_{0.04}\text{O}_2$ nanoparticles.

The emission spectra partitioned into three fundamental extents, portrayed by the accompanying qualities: the initial segment comprises of a sharp ultraviolet band situated at 357 nm (3.47 eV) because of the natural deformities in SnO_2 nanoparticles. A subsequent district incorporates discharge groups around 488, and their bandgap energy is 2.54 eV. These violet and blue band emission have created by the recombination of profoundly caught charges and photogenerated electrons from the conduction band. Broad green emission band retained at 532 nm (2.33 eV) can ascribe to radiative recombination from an imperfection, for example, oxygen vacancies [40].

4. Conclusion

By using a straightforward Co-precipitation technique, pure SnO_2 and $\text{Sn}_{0.94}\text{Cu}_{0.02}\text{Zn}_{0.04}\text{O}_2$ nanoparticles were effectively created. PXRD spectroscopy validated the structural analyses. Where the $\text{Sn}_{0.94}\text{Cu}_{0.02}\text{Zn}_{0.04}\text{O}_2$ nanoparticles' crystallite size drops, this indicates that the Cu and Zn ions were effectively doped into pure SnO_2 nanoparticles. By using SEM analysis, morphological alterations were detected. Compared to pure SnO_2 , $\text{Sn}_{0.94}\text{Cu}_{0.02}\text{Zn}_{0.04}\text{O}_2$ nanoparticles have a more restricted structure. Again, the lack of contaminants found by EDAX analysis demonstrates that our dopant ions were successfully incorporated into pure SnO_2 nanoparticles. By using FTIR spectroscopy, functional group analyses were carried out. Significant emission at 357 nm was shown by PL tests, although it became less intense as dopants were added to the pure SnO_2 nanoparticles. In summary, the effect of adding (Cu-2%, Zn-4%) into pure SnO_2 nanoparticles brings reduce in crystalline size, makes changes in morphological shapes, and shows intensity reduction in PL spectroscopy and the prepared nanoparticles will be suitable for spintronics and optical instrumentations.

5. References

- [1]. Muthukumar, Harshiny, and ManickamMatheswaran. "Amaranthusspinosus leaf extract mediated FeO nanoparticles: physicochemical traits, photocatalytic and antioxidant activity." *ACS Sustainable Chemistry & Engineering* 3, no. 12 (2015): 3149-3156.
- [2]. Sugimoto, T., Zhou, X., & Muramatsu, A. (2002). Synthesis of uniform anatase TiO₂ nanoparticles by gel-sol method: 1. Solution chemistry of Ti (OH)ⁿ (4- n)⁺ complexes. *Journal of Colloid and Interface Science*, 252(2), 339-346.
- [3]. Dagher, Sawsan, Yousef Haik, Ahmad I. Ayesh, and Nacir Tit. "Synthesis and optical properties of colloidal CuO nanoparticles." *Journal of Luminescence* 151 (2014): 149-154.
- [4]. Kawasaki, S. I., Sue, K., Ookawara, R., Wakashima, Y., Suzuki, A., Hakuta, Y., & Arai, K. (2010). Engineering study of continuous supercritical hydrothermal method using a T- shaped mixer: Experimental synthesis of NiO nanoparticles and CFD simulation. *The Journal of Supercritical Fluids*, 54(1), 96-102.
- [5]. Aziz, Madzlan, SaadSaber Abbas, and Wan Rosemaria Wan Baharom. "Size-controlled synthesis of SnO₂ nanoparticles by sol-gel method." *Materials Letters* 91 (2013): 31-34.
- [6]. Yousefi, Ramin, Ali Khorsand Zak, FaridJamali-Sheini, Nay Ming Huang, Wan JeffreyBasirun, and M. Sookhakian. "Synthesis and characterization of single crystal PbO nanoparticles in a gelatin medium." *Ceramics International* 40, no. 8 (2014): 11699-11703. [7]. Huang, Xing, Yong-Qiang Yu, Jing Xia, Hua Fan, Lei Wang, Marc-Georg Willinger, Xiao- Ping Yang, Yang Jiang, Tie-Rui Zhang, and Xiang-Min Meng. "Ultraviolet photodetectors with high photosensitivity based on type-II ZnS/SnO₂ core/shell heterostructured ribbons." *Nanoscale* 7, no. 12 (2015): 5311-5319.
- [8]. Jiang, L., Sun, G., Zhou, Z., Sun, S., Wang, Q., Yan, S., ...& Xin, Q. (2005). Size-controllable synthesis of monodispersed SnO₂ nanoparticles and application in electrocatalysts. *The Journal of Physical Chemistry B*, 109(18), 8774-8778.
- [9]. Hülser, T. P., H. Wiggers, F. E. Kruis, and A. Lorke. "Nanostructured gas sensors and electrical characterization of deposited SnO₂ nanoparticles in ambient gas atmosphere." *Sensors and Actuators B: Chemical* 109, no. 1 (2005): 13-18.
- [10]. Song, Tze-Bin, and Ning Li. "Emerging transparent conducting electrodes for organic light emitting diodes." *Electronics* 3, no. 1 (2014): 190-204.
- [11]. Chen, W., Qiu, Y., Zhong, Y., Wong, K. S., & Yang, S. (2010). High-efficiency dye-sensitized solar cells based on the composite photoanodes of SnO₂ nanoparticles/ZnO nanotetrapods. *The Journal of Physical Chemistry A*, 114(9), 3127-3138.
- [12]. Lou, Xiong Wen, Yong Wang, Chongli Yuan, Jim Yang Lee, and Lynden A. Archer. "Template-free synthesis of SnO₂ hollow nanostructures with high lithium storage capacity." *Advanced Materials* 18, no. 17 (2006): 2325-2329.
- [13]. Wang, Yude D., Igor Djerdj, Markus Antonietti, and Bernd Smarsly. "Polymer-assisted generation of antimony-doped SnO₂ nanoparticles with high crystallinity for application in gas sensors." *Small* 4, no. 10 (2008): 1656-1660.
- [14]. Paraguay-Delgado, F., W. Antúnez-Flores, M. Miki-Yoshida, A. Aguilar-Elguezabal, P. Santiago, R. Diaz, and J. A. Ascencio. "Structural analysis and growing mechanisms for long SnO₂ nanorods synthesized by spray pyrolysis." *Nanotechnology* 16, no. 6 (2005): 688.
- [15]. Wang, Luyuan Paul, et al. "Novel Preparation of N-Doped SnO₂ Nanoparticles via Laser-Assisted Pyrolysis: Demonstration of Exceptional Lithium Storage Properties." *Advanced materials* 29.6 (2017): 1603286.
- [16]. Gnanam, S., and V. Rajendran. "Luminescence properties of EG-assisted SnO₂ nanoparticles by sol-gel process." *Digest Journal of Nanomaterials and Biostructures* 5.3 (2010): 699-704.

- [17]. Lu, Geyu, et al. "UV-enhanced room temperature NO₂ sensor using ZnO nanorods modified with SnO₂ nanoparticles." *Sensors and Actuators B: Chemical* 162.1 (2012): 82-88.
- [18]. Shaikh, F. I., et al. "Facile Co-precipitation synthesis and ethanol sensing performance of Pd loaded Sr doped SnO₂ nanoparticles." *Powder Technology* 326 (2018): 479-487.
- [19]. Chen, Deliang, and Lian Gao. "Novel synthesis of well-dispersed crystalline SnO₂ nanoparticles by water-in-oil microemulsion-assisted hydrothermal process." *Journal of colloid and interface science* 279.1 (2004): 137-142.
- [20]. Zhong, Xiaohua, et al. "Effect of calcining temperature and time on the characteristics of Sb-doped SnO₂ nanoparticles synthesized by the sol-gel method." *Particuology* 10.3 (2012): 365-370.
- [21]. Sagadevan, Suresh, et al. "Cu-doped SnO₂ nanoparticles: synthesis and properties." *Journal of nanoscience and nanotechnology* 19.11 (2019): 7139-7148.
- [22]. Asaithambi, S., et al. "Influence of Ni Doping in SnO₂ Nanoparticles with Enhanced Visible Light Photocatalytic Activity for Degradation of Methylene Blue Dye." *Journal of nanoscience and nanotechnology* 19.8 (2019): 4438-4446.
- [23]. Almamoun, Omer, and Shu Yi Ma. "Effect of Mn doping on the structural, morphological and optical properties of SnO₂ nanoparticles prepared by Sol-gel method." *Materials Letters* 199 (2017): 172-175.
- [24]. Cabrera, A. F., et al. "Mechanosynthesis of Fe-doped SnO₂ nanoparticles." *Physica B: Condensed Matter* 398.2 (2007): 215-218.
- [25]. Chen, Weibing, and Jingbo Li. "Magnetic and electronic structure properties of Co-doped SnO₂ nanoparticles synthesized by the sol-gel-hydrothermal technique." *Journal of Applied Physics* 109.8 (2011): 083930.
- [26]. Sun, Peng, et al. "One-step synthesis and gas sensing properties of hierarchical Cd-doped SnO₂ nanostructures." *Sensors and Actuators B: Chemical* 190 (2014): 32-39.
- [27]. Wu, Ping, Baozeng Zhou, and Wei Zhou. "Room-temperature ferromagnetism in epitaxial Mg-doped SnO₂ thin films." *Applied Physics Letters* 100.18 (2012): 182405.
- [28]. Nachiar, R. Ariya, and S. Muthukumar. "Structural, photoluminescence and magnetic properties of Cu-doped SnO₂ nanoparticles co-doped with Co." *Optics & Laser Technology* 112 (2019): 458-466.
- [29]. Zhang, Shumin, et al. "Facile fabrication of a well-ordered porous Cu-doped SnO₂ thin film for H₂S sensing." *ACS applied materials & interfaces* 6.17 (2014): 14975-14980.
- [30]. Holzwarth, Uwe, and Neil Gibson. "The Scherrer equation versus the 'Debye-Scherrer equation'." *Nature nanotechnology* 6.9 (2011): 534-534.